Supporting Information
Quenching Pathways in $NaYF_4$:Er^{3+},Yb^{3+} Upconversion Nanocrystals

Freddy T. Rabouw, P. Tim Prins, Pedro Villanueva-Delgado,
Marieke Castelijns, Robin G. Geitenbeek, and Andries Meijerink
Debye Institute for Nanomaterials Science, Utrecht University,
Princetonplein 1, 3584 CC Utrecht, The Netherlands

Table S1 | Composition and sizes of the doped $NaYF_4$ nanocrystals (NCs) used in our experiments. Elemental compositions are determined using inductively coupled plasma atomic emission spectroscopy. Diameters of (quasi-)spherical core-only NCs are given as the mean ± standard deviation over > 100 measurements on transmission electron micrographs. The core–shell NCs are slightly elongated (Figure S1). Their dimensions are given as mean ± standard deviation for the longest and the shortest axis over > 100 measurements. The 'average shell thickness' is then calculated as the average between the shell thickness (*i.e.*, mean core–shell NC size minus mean core-only NC diameter) in the long direction and in the short direction. In our solvent-quenching modeling and analysis, the different sizes of NCs with different dopant concentrations are taken into account. Each NC sample is approximated as being perfectly monodisperse, where the NCs have spherical core with a diameter equal to the mean diameter of the sample and are covered by an isotropic non-luminescent shell with the 'average shell thickness'.

Nominal composition	Actual composition	Core diameter (nm)	Core–shell dimensions (nm)	Average shell thickness (nm)
0.1% Er^{3+}	0.1% Er^{3+}	19.3 ± 1.1	27.2 ± 1.8 21.4 ± 1.7	2.5
2% Er^{3+}	1.7% Er^{3+}	18.6 ± 0.9	26.3 ± 2.1 22.1 ± 2.4	2.8
2% Er^{3+} / 18% Yb^{3+}	1.7% Er^{3+} / 18.0% Yb^{3+}	21.6 ± 0.9	28.6 ± 1.7 23.5 ± 1.6	2.2
18% Yb^{3+}	17.5% Yb^{3+}	22.1 ± 1.1	28.6 ± 2.2 24.5 ± 2.0	2.2
0.1% Yb^{3+}	0.1% Yb^{3+}	18.1 ± 0.9	28.7 ± 1.7 23.6 ± 2.1	4.0

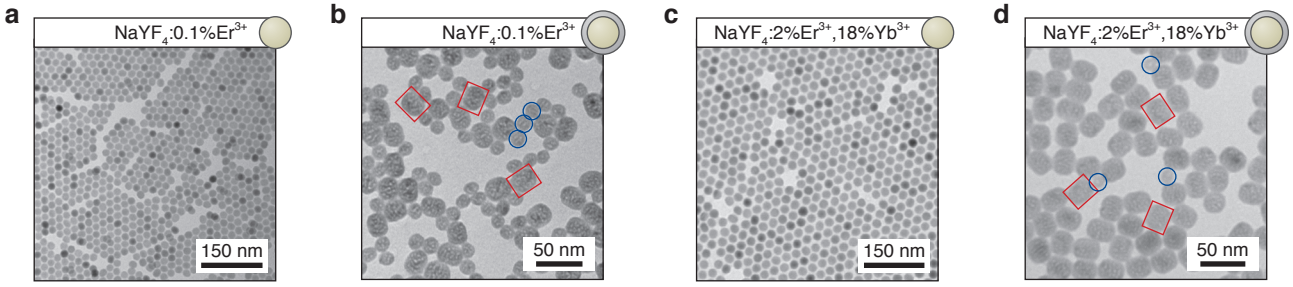

Figure S1 | Transmission electron micrographs of the nanocrystals (NCs) used in our experiments. **(a,b)** $NaYF_4$ NCs doped with 0.1% Er^{3+}, **(a)** before and **(b)** after growth of a non-luminescent $NaYF_4$ shell. After shell growth the sample contains core–shell NCs with a rectangular shape (three examples highlighted in red in **b**) as well as small round particles due to secondary nucleation (highlighted in blue). The small secondary particles are undoped and therefore non-luminescent. They are not further considered in the statistical analysis of the particle dimensions (see Table S1 above). **(c,d)** Same, but for $NaYF_4$ NCs co-doped with 2% Er^{3+} and 18% Yb^{3+}.

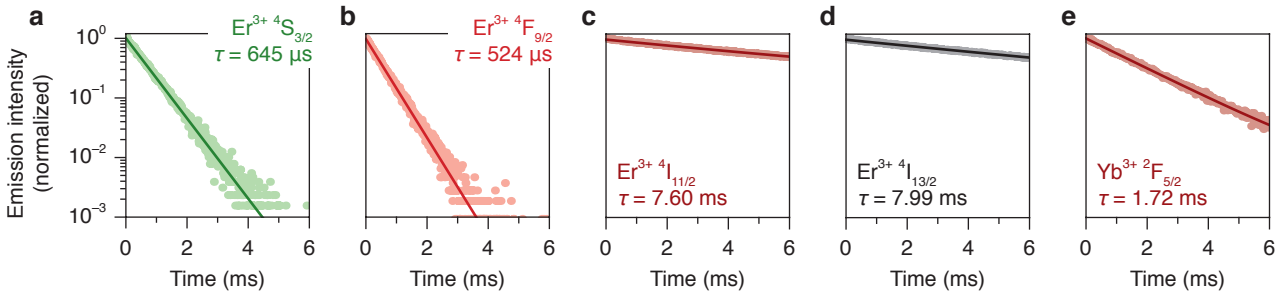

Figure S2 | Photoluminescence decay dynamics of **(a)** the green-emitting $^4S_{3/2}$ excited state, **(b)** the red-emitting $^4F_{9/2}$ excited state, **(c)** the near-infrared-emitting $^4I_{11/2}$ excited state, and **(d)** the mid-infrared-emitting $^4I_{13/2}$ excited state in β-$NaYF_4$ microcrystalline powder doped with 0.1% Er^{3+}, and of **(e)** the near-infrared-emitting $^2F_{5/2}$ excited state in bulk β-$NaYF_4$ microcrystalline powder doped with 0.01% Yb^{3+}. All curves can be fitted to a single-exponential decay function, from which we extract the excited-state lifetimes as indicated in the plots. The low dopant concentrations minimize quenching by cross-relaxation and energy migration. Furthermore, we minimize reabsorption by diluting the sample with non-luminescent $BaSO_4$ powder. The fitted time constants are therefore good estimates for the radiative lifetimes of the excited states.

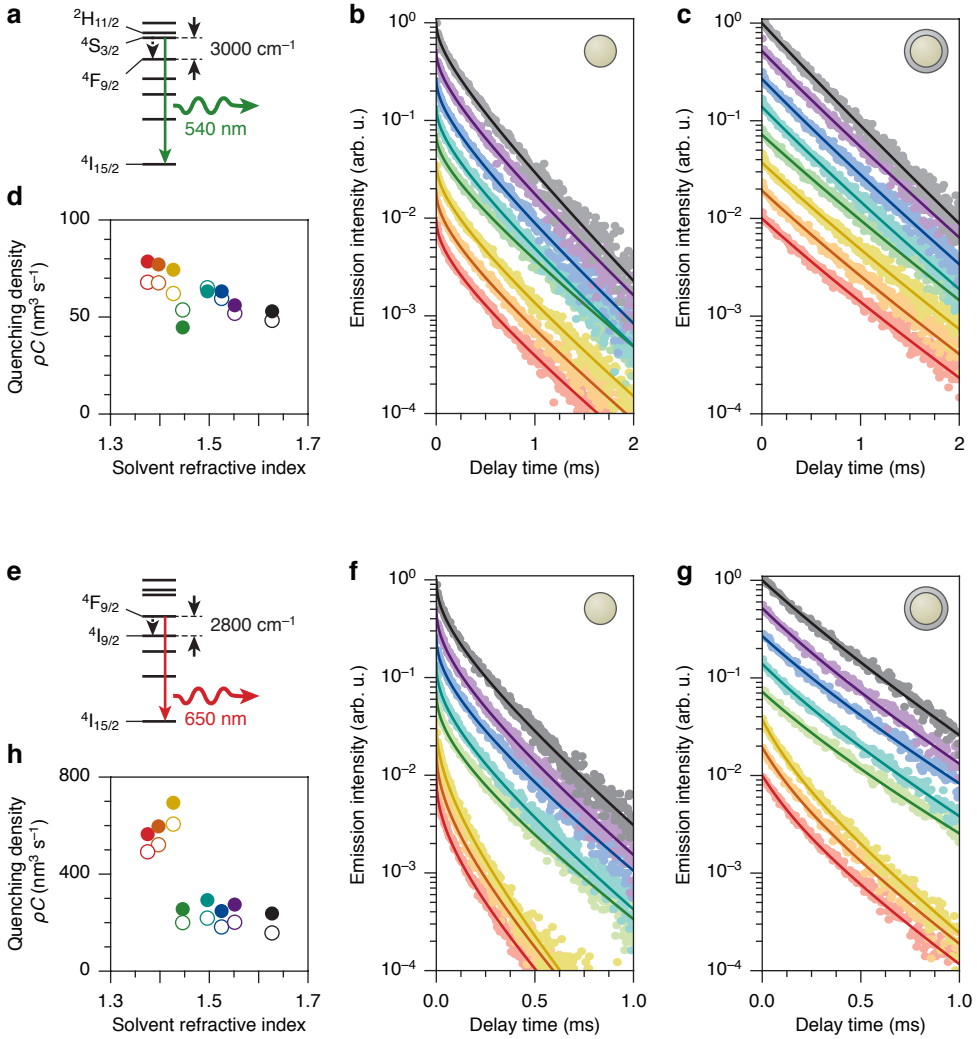

Figure S3 | Solvent quenching of **(a–d)** the green-emitting $^4S_{3/2}$ and $^2H_{11/2}$ levels, and **(e–h)** the red-emitting $^4F_{9/2}$ level. **(a,e)** The energy level structure of Er^{3+} showing the radiative transitions to the ground state as colored arrows, and nonradiative transitions from one level to the next lower level as black arrows. The energy gaps for the nonradiative transitions are indicated. **(b,f)** Photoluminescence decay curves of core-only $NaYF_4$:0.1% Er^{3+} nanocrystals and of **(c,g)** $NaYF_4$:0.1% Er^{3+}/$NaYF_4$ core–shell nanocrystals dispersed in various solvents: hexane (red), octane (orange), cyclohexane (yellow), chloroform (green), toluene (cyan), chlorobenzene (blue), *o*-dichlorobenzene (purple), and carbon disulfide (black). Solid lines are fits to $I(t) = AR(t)Q(t)$ (eq 5 in the main text), with A the overall signal amplitude, $R(t)$ describing radiative decay, and $Q(t)$ solvent quenching (see main text for details). Each fit optimizes the amplitude A and the solvent quenching density ρC, while the radiative decay rate γ_{rad} is fixed based on the bulk decay rate (Figure S2) and nanocrystal-cavity model for the effect of the solvent refractive index (eq 3 in the main text). **(d,h)** Values of the solvent quenching density ρC for the different solvents (different colors), extracted from the decay dynamics of Er^{3+} in core-only nanocrystals (filled circles) and core–shel nanocrystals (open circles).

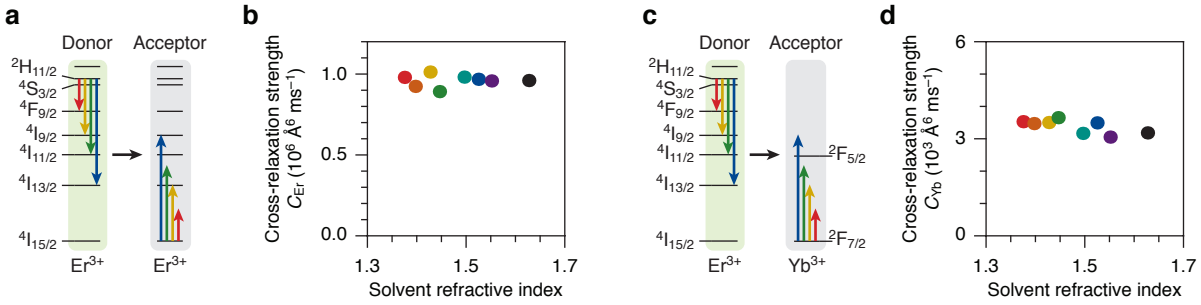

Figure S4 | **(a)** Schematic of cross-relaxation pathways for the green-emitting levels of Er^{3+} ($^2H_{11/2}$ and $^4S_{3/2}$) transferring part of their energy to a neighboring Er^{3+} ion in the ground state. **(b)** Cross-relaxation strengths C_{Er} for this process, obtained by fitting experimental decay curves of the green luminescence from core–shell NCs with 2% Er^{3+} doping in the core and dispersed in various solvents (x-axis) to our model for radiative decay, solvent quenching, and cross-relaxation (eq 8 in the main text). The reduced-chi-squared values, indicating the fit quality, are $\chi^2_{red} = 1.17 \pm 0.18$ (mean ± standard deviation for the different solvents) yielding cross-relaxation strengths of $C_{Er} = (9.6 \pm 0.4) \times 10^5$ Å^6 ms^{-1}. **(c,d)** Same for cross-relaxation to neighboring Yb^{3+} ions, studied on core–shell NCs with the core containing 2% Er^{3+} and 18% Yb^{3+}, and modeled using eq 10 in the main text. We obtain $\chi^2_{red} = 1.09 \pm 0.06$ and $C_{Yb} = (3.4 \pm 0.2) \times 10^3$ Å^6 ms^{-1}.

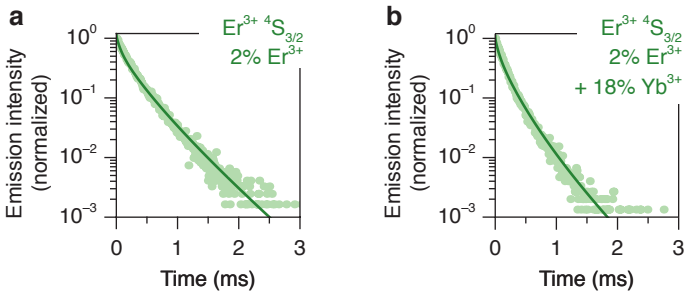

Figure S5 | Photoluminescence decay curves of the green emission from the Er^{3+} $^4S_{3/2}$ level in bulk $NaYF_4$ **(a)** doped with 2% Er^{3+}, or **(b)** co-doped with 2% Er^{3+} and 18% Yb^{3+}. The solid lines are fits to our model of radiative decay plus cross-relaxation (eq 8 and eq 10 in the main text), where the cross-relaxation strengths C_{Er} and C_{Yb} are fixed based on the fit results from core–shell NCs dispersed in toluene (Figure 3f in the main text). The solvent-quenching strength ρC is set to zero, because we consider bulk material here. The model matches the experimental data very well without fit parameters.

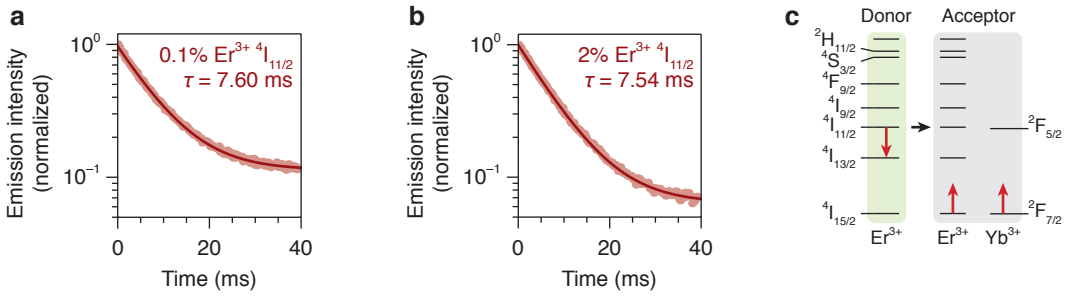

Figure S6 | **(a)** Photoluminescence decay curve of the near-infrared emission from the Er^{3+} $^4I_{11/2}$ level in bulk $NaYF_4$ doped with 0.1%. The solid line is a fit to a single exponential plus background, yielding a lifetime of 7.60 ms. **(b)** Same for 2% Er^{3+} doping, with a lifetime of 7.54 ms. **(c)** Cross-relaxation pathways from the Er^{3+} $^4I_{11/2}$ level to neighboring Er^{3+} or Yb^{3+} ions in the ground state. No energy-conserving pathway is possible.